Journal of Thermal Analysis, Vol. 34 (1988) 37–45

DEHYDRATION KINETICS OF HYDRATED IRON OXIDE FROM DYNAMIC THERMOGRAVIMETRY

N. Sh. Petro and *B. S. Girgis*

SURFACE CHEMISTRY LABORATORY, NATIONAL RESEARCH CENTRE, DOKKI, CAIRO, EGYPT

(Received October 20, 1986; in revised form April 14, 1987)

The thermal treatment of $Fe_2O_3 \cdot 1.65H_2O$ gives rise to sharp dehydration weight-change waves (310–470 K and 470–670 K) which correspond to the loss of loosely-bound and strongly-bound water, respectively. Analysis of the thermal waves was performed by the method of Šatava and Škvara (1969), the modified method of Coats and Redfern (1964) and the method of Blazejowski et al. (1983), and by applying a least squares straight line fit to the data. The A_2 and A_3 decomposition mechanisms predominate in the first dehydration step, whereas an F_1 mechanism seems the best to describe dehydration of the structural water. Activation energies of 21 $kJ \cdot mol^{-1}$ and 95 $kJ \cdot mol^{-1}$ are estimated for the first and second steps, respectively.

The analysis of thermogravimetric curves has been the subject of a large number of publications [1–16]. It aims at deriving certain kinetic parameters from a single TG curve. These are: order and mechanism of reaction, activation energy and Arrhenius frequency factor.

To describe the rate of weight change, several expressions have been used to cover different solid-state decomposition mechanisms, e.g. phase boundary-controlled processes, nucleation processes, nucleation followed by linear or bulk growth of nuclei, or diffusion-controlled processes. The most predominant or probable mechanism would be that which satisfies optimization of the fractional weight-change data throughout the whole range of temperature considered.

The thermal analysis of hydrated iron oxide has been reported by some authors [17, 18]. Loss of water usually occurs in two temperature ranges, giving a low-temperature effect and a high temperature effect. The former is attributed to the loss of physically adsorbed water (loosely bound), and the latter to the loss of structural water (strongly bound). However, a distinction between these two categories can be made not only via their positions in the TG or DTA curves, but also through the activation energy associated with each dehydration.

John Wiley & Sons, Limited, Chichester
Akadémiai Kiadó, Budapest

Dynamic thermogravimetry of an ion-free hydrated iron oxide is employed in the present investigation for the purpose of distinguishing between the two stages of dehydration. Possible differences in the mechanisms of dehydration and the activation energies are illustrated.

Experimental

Iron oxide hydrate was prepared by the addition of dilute ammonium hydroxide (20%) to an equal volume of 30% iron(III) chloride. The precipitate was washed several times by decantation with the same dilute ammonia solution, but still contained chloride ions. It was therefore washed with hot ($\sim 80°$) 50% NH_4OH till chloride-free washings were attained, and then with water till the washings were neutral and ammonium ion-free, and finally dried at 50°. Chemical analysis gave the structural formula $Fe_2O_3 \cdot 1.65H_2O$.

This procedure is intended to eliminate completely foreign ions that may cause complications by giving rise to abnormal dehydration waves.

Weight-loss analysis was carried out with an apparatus produced by Netzsch Gerätebau GmBH, Selb, West Germany, at a heating rate of 5 deg min^{-1}.

Theoretical basis for analysis

The ultimate aim of analysing dynamic TG traces is to linearize the data in the form of the decomposition fraction (α) as a function of temperature T. Certain well-established kinetic solid-state equations are employed to describe the TG wave, and are associated with one or more rate-determining mechanisms. In the present study three general methods are used in association with nine of the currently employed mechanisms. For all procedures of analysis, a least squares fit for a straight line has been employed and the corresponding correlation coefficient, r and standard error of deviation S_e were estimated in every case.

1. The method of Šatava and Škvara (ŠŠ)

According to these authors [12], $\log g(\alpha)$ is plotted vs. $\frac{1}{T}$ for each of the nine solid-state decomposition mechanisms (D_1, D_2, D_3, D_4, F_1, A_2, A_3, R_2 and R_3). From the slope of the best straight line, extending over the whole range of decomposition, the heat of activation (E_a) associated with the process is calculated from the approximate formula given by Šatava [7]:

$$E_a = -\tan\beta + \sqrt{\tan^2\beta + 8\tan\beta \cdot T} \qquad (1)$$

where $\tan \beta$ is the slope of the straight line; and T is the temperature corresponding to 50% decomposition. The values given by Šatava and Škvara [12] for $\log g(\alpha)$ are used.

2. The method of Coats and Redfern (CR)

In the original method [2], the authors assumed a first-order reaction mechanism, as well as fractional orders down to zero. Their expressions appear as:

$$\log\left[\frac{1-(1-\alpha)^{1-n}}{T^2}\right] = \log\left[\frac{AR}{\Phi E_a}\left(1-\frac{2RT}{E_a}\right)\right] - \frac{E_a}{2.3RT} \quad (\text{for } n \neq 1) \tag{2}$$

and

$$\log\left[\frac{-\ln(1-\alpha)}{T^2}\right] = \log\left[\frac{AR}{\Phi E}\left(1-\frac{2RT}{E_a}\right)\right] - \frac{E_a}{2.3RT} \quad (\text{for } n = 1) \tag{3}$$

In recent years, the method has been modified and extended to cover all of the nine currently accepted solid-state reaction mechanisms [16, 19, 20]. The general equation thus appears in the form:

$$\log\left[\frac{g(\alpha)}{T^2}\right] = \log\left[\frac{AR}{\Phi E_a}\right] - \frac{E_a}{2.3RT} \tag{4}$$

or

$$\log\left[\frac{g(\alpha)}{T^2}\right] = \log\left[\frac{AR}{\Phi E}\left(1-\frac{2RT}{E_a}\right)\right] - \frac{E_a}{2.3RT} \tag{5}$$

Where T is the absolute temperature at the specified fraction; R is the gas constant; Φ is the linear rate of heating; and A is the Arrhenius frequency factor. If the correct $g(\alpha)$ is used, a plot of the left-hand side of the equation versus $1/T$ should give a straight line, from which the values of E and A could be estimated.

3. The method of Blazejowski et al. (Blz)

These authors derived another relationship, which was found applicable to certain solid-state reaction kinetics [16, 21]. The logarithm of the integral equation appears in the form

$$\log\frac{g(\alpha)}{T} = \log\frac{A}{\Phi} - \frac{E_a}{2.3RT} \tag{6}$$

which was found to be suitable in the linearization procedure. The values of E_a and A are similarly easily evaluated.

Results

The TG curve of iron oxide hydrate is plotted in Fig. 1; it exhibits two distinctly separated dehydration waves. It differs from previously published results [18]. The clearly separated dehydration stages could be due to the elaborate method of preparing the present solid, and to its considerable aging in solution, which leads to a well-crystallized hydrated oxide. Step I of the dehydration, which ends at 470 K, involves a loss of 6.7% (0.652 mole H_2O), while step II, from this temperature up to 670 K, involves a loss of 8.25% (0.861 mole H_2O). The two dehydration waves were transformed into kinetic curves (Fig. 2) and plotted as percentage dehydration as a function of temperature.

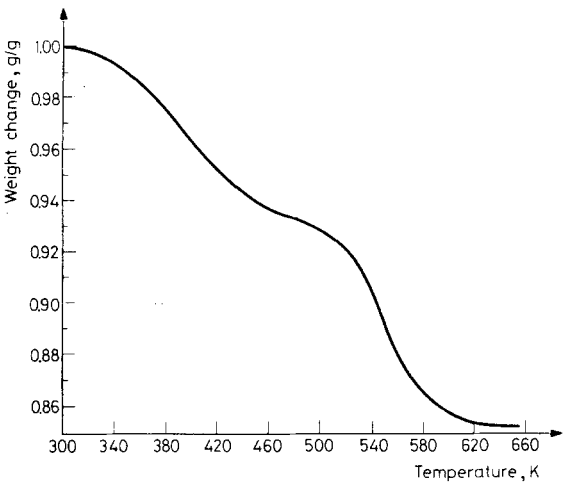

Fig. 1 Thermogravimetric curve of iron oxide hydrate

First dehydration step

Comparison of the data in Table 1 indicates that the three methods of analysis yield activation energies that vary by about ±10–15%. The most favourable method for analysis is the ŠŠ method, because it gives the best fit to dehydration, as indicated by the highest correlation coefficients and lowest standard errors of the estimate. This same method invariably gives the highest activation energies, whereas the CR method yields the lowest values.

The different decomposition mechanisms lead to an almost 10-fold variation in both E_a and $\log A$. With respect to the method, the highly probable mechanisms that describe dehydration are the A_2 and A_3 ones. This is associated with a mean value of E_a and $\log A$. With respect to the ŠŠ method, the highly probable

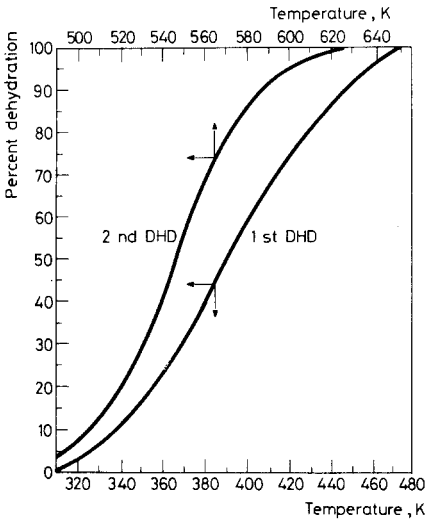

Fig. 2 Percent decomposition as function of temperature for the first and second dehydration (DHD) steps of iron oxide hydrate

mechanisms that describe dehydration are the A_2 and A_3 ones. This is associated with a mean value of $E_a = 21$ kJ mol^{-1}. The most unfavourable mechanisms are those controlled by diffusion (D_1, D_2, D_3 and D_4).

The modified CR method indicates that dehydration is best described by a D_2 mechanism ($E_a = 51.6$ kJ mol^{-1}, $r = 0.985632$ and $S_e = 20.8 \times 10^{-2}$). The Blz method shows that all of the decomposition mechanisms fit equally to a straight line, with small variations in either r or S_e. However, the best of these straight lines corresponds to the first-order mechanism (F_1) with an activation energy of 33.3 kJ·mol^{-1} ($r = 0.981126$, $S_e = 8.57 \times 10^{-2}$).

Second dehydration step

Table 2 lists the kinetic parameters evaluated by applying the three outlined analysis procedures to the dehydration wave extending from 470 to 670 K. It is to be mentioned that all of the three prescribed methods of TG curve analysis apply equally well to this principal dehydration, as evident from the small differences between the highest and lowest correlation coefficients (0.994364 and 0.962027). This is true irrespective of the kinetic equation employed. An apparent and substantial difference appears in the standard error of the estimate (ca. 12-fold) but there is only a 6-fold change in the evaluated activation energies. The D_3 mechanism invariably yields the highest activation energies, and the A_3 mechanism the lowest values (ratio 6 : 1). Two methods (CR and Blz) give activation energies

Table 1 Kinetic parameters of dehydration of iron oxide hydrate in the range 310–470 K

Mechanism	Method	E_a (kJ·mol^{-1})	r	$S_e \times 10^2$	log A
D_1	ŠŠ	59.8	0.965081	19.4	
	CR	46.1	0.939131	22.0	4.689
	Blz	49.9	0.955975	20.0	4.002
D_2	ŠŠ	65.4	0.981748	14.9	
	CR	51.6	0.985632	20.8	5.279
	Blz	55.2	0.967856	18.8	4.522
D_3	ŠŠ	72.3	0.986422	14.3	
	CR	58.5	0.968914	19.5	5.738
	Blz	62.2	0.978631	17.1	4.931
D_4	ŠŠ	69.5	0.981117	6.94	
	CR	53.4	0.954230	21.9	4.933
	Blz	57.4	0.970828	18.5	4.207
F_1	ŠŠ	42.3	0.980703	9.5	
	CR	29.6	0.963504	10.8	2.891
	Blz	33.3	0.981126	8.57	2.349
A_2	ŠŠ	23.9	1.00000	2.29	
	CR	11.2	0.912235	6.53	0.174
	Blz	14.8	0.962124	5.47	0.022
A_3	ŠŠ	17.2	0.998549	0.87	
	CR	7.0	0.882762	6.23	−0.857
	Blz	8.7	0.945001	3.93	−0.799
R_2	ŠŠ	37.0	0.983323	7.54	
	CR	23.9	0.912316	11.6	1.648
	Blz	27.6	0.963625	9.98	1.88
R_3	ŠŠ	38.9	0.987104	5.9	
	CR	23.1	0.847394	8.8	1.363
	Blz	29.2	0.968240	9.98	1.271

with only slight differences, whereas about 10% higher values result from the ŠŠ method. Linearization of the second dehydration wave is best described by the F_1, A_2 and A_3 mechanism, with a high mean correlation coefficient, $r = 0.990341$, and a low dispersion of the data, $S_e = 3.22$ for all procedures. The activation energy cannot be evaluated in the form of a mean value, since it is approximately linearly dependent on $1/n$ in the Avrami–Erofeev equations. Nevertheless, on the basis of the best linear fit, as represented by the highest correlation coefficient (F_1 mechanism), the activation energy of dehydration in the second stage would be ~ 95 kJ·mol^{-1}.

Table 2 Kinetic parameters of dehydration of iron oxide hydrate in the range 470–670 K

Mechanism	Method	E_a, kJ·mol^{-1}	$-r$	$S_e \times 10^2$	log A
D_1	ŠŠ	146.7	0.965026	22.53	
	CR	128.0	0.969335	19.14	10.91
	Blz	132.5	0.962027	19.22	9.86
D_2	ŠŠ	160.0	0.970741	19.02	
	CR	142.1	0.971895	17.48	12.09
	Blz	146.5	0.970902	17.38	11.01
D_3	ŠŠ	179.6	0.988012	13.47	
	CR	160.5	0.985296	14.14	13.39
	Blz	165.0	0.986066	14.15	12.24
D_4	ŠŠ	156.9	0.979840	23.72	
	CR	148.3	0.976786	16.49	12.06
	Blz	152.4	0.977522	16.75	10.96
F_1	ŠŠ	103.9	0.994364	3.14	
	CR	85.8	0.992208	5.49	7.28
	Blz	90.4	0.992183	5.77	6.40
A_2	ŠŠ	55.6	0.993944	2.69	
	CR	38.4	0.989698	2.84	2.53
	Blz	42.9	0.992271	2.73	1.96
A_3	ŠŠ	39.2	0.994357	1.72	
	CR	22.3	0.974479	2.61	0.84
	Blz	26.8	0.989566	1.98	0.45
R_2	ŠŠ	89.1	0.9818816	7.86	
	CR	70.4	0.967020	9.43	5.34
	Blz	75.7	0.979240	7.57	4.39
R_3	ŠŠ	101.9	0.986009	7.27	
	CR	75.6	0.982556	7.28	5.78
	Blz	80.2	0.984793	7.19	4.89

The compensation effect

It has long been reported that a linear relationship holds between the two kinetic parameters evaluated from the thermal curves, i.e. E_a and log A [10, 22, 23].

This intercorrelation, or effect, has been denoted the kinetic compensation effect, and can furnish additional information about the decomposition process [23]. The linear representation of this appears in the form

$$\log A = aE + b \tag{7}$$

The logarithms of the preexponential factors, $\log A$, have been calculated from the intercepts of Eqs (4), (5) and (6), and the values are listed in Tables 1 and 2. The values calculated with the two expressions (4) and (5) of the Coats and Redfern equation are indistinguishable. A least squares straight line fit was applied to the values, and the compensation effect appears in the following equations.

For the first dehydration stage:

$$\log A = 0.1140\ E_a - 1.429 \qquad (r = 0.966602,\ S_e = 58 \times 10^{-2}) \tag{8}$$

and for the second dehydration stage:

$$\log A = 0.0871\ E - 1.249 \qquad (r = 0.984973,\ S_e = 76 \times 10^{-2}) \tag{9}$$

These relations would become more significant upon variation of the conditions of measuring the TG wave of this hydrated iron oxide system.

In conclusion, the tested iron oxide hydrate exhibited two distinctly separated dehydration TG waves. The second weight loss is associated with dehydroxylation and shows a 5-fold higher activation energy in comparison with the simple dehydration of adsorbed water.

References

1 E. S. Freeman and B. Carroll, J. Phys. Chem., 62 (1958) 394.
2 C. D. Doyle, J. Appl. Polym. Sci., 5 (1961) 285.
3 V. Šatava, Silikaty (Prague) 5 (1961) 68.
4 H. H. Horowitz and G. Metzger, Anal. Chem., 35 (1963) 1464.
5 A. W. Coats and J. P. Redfern, Nature, 201 (1964) 68.
6 B. N. N. Achar, G. W. Brindley and J. H. Sharp, Proc. Int. Clay Conf., Jerusalem, 1 (1966) 67.
7 J. Šestak, Silikaty, 11 (1967) 153.
8 J. Zsakó, J. Phys. Chem., 72 (1968) 2406.
9 V. Šatava and F. Škvara, J. Am. Ceram. Soc., 52 (1969) 591.
10 J. R. MacCallum and J. Tanner, European Polym. J., 6 (1970) 1033.
11 V. Šatava, Thermochim. Acta, 2 (1971) 423.
12 J. Šestak and G. Berggren, Thermochim. Acta, 3 (1971) 1.
13 J. Zsakó, J. Thermal Anal., 5 (1973) 239.
14 J. Blazejowski, J. Szychinski and E. Kowalewska, Thermochim. Acta, 66 (1983) 197.
15 F. Martin, A. Gonzalez, J. Jimenez, J. Largo and J. A. de Saja, J. Thermal Anal., 29 (1984) 257.
16 J. P. Elder, Analytical Calorimetry, Ed. J. F. Johnson and P. S. Gill, Plenum Publishing Corp. 1984, p. 255.
17 B. R. Arora, N. K. Mandal, R. L. Chowdhury, N. G. Ganguli and S. P. Sen, Technology, 9 (1972) 143.
18 A. Spinzi and I. V. Nicolescu Rev. Romaine de Chim., 20 (1975) 387.

19 H. Tanaka and M. Tokumitsu, J. Thermal Anal., 29 (1984) 87.
20 A. M. Gadalla, Int. J. Chem. Kint., 16 (1984) 1471.
21 J. Blazejowski, Thermochim. Acta, 48 (1981) 109.
22 J. Zsakó and H. E. Arz, J. Thermal Anal., 6 (1974) 651.
23 Z. Adonyi and G. Körösi, Thermochim. Acta, 60 (1983) 23.

Zusammenfassung — Bei der thermischen Behandlung von $Fe_2O_3 \cdot 1.65H_2O$ werden zwei der Abgabe von schwach bzw. stark gebundenem Wasser zuzuschreibende Gewichtsveränderungen bei 310–470 K und 470–670 K festgestellt. Die Analyse der thermischen Kurven wurde nach der von Coats und Redfern (1964) und Blazejowski et al. (1983) modifizierten Methode von Šatava und Škvara (1969) ausgeführt und die Korrelation der Daten nach der Methode der kleinsten Fehlerquadrate berechnet. Die Zersetzungsmechanismen A_2 und A_3 dominieren im ersten Dehydratisierungsschritt, während die Abgabe von strukturellem Wasser am besten durch den F_1-Mechanismus zu beschreiben ist. Für den ersten und zweiten Schritt wurden Aktivierungsenergien von 21 bzw. 95 $kJ \cdot mol^{-1}$ ermittelt.

Резюме — Термическая обработка $Fe_2O_3 \cdot 1{,}65H_2O$ показала наличие двух резких пиков дегидратации при 310–470 K и 470–670 K, что соответствует потери слабосвязанной и сильносвязанной воды. Анализ термических кривых проведен методом Шатавы и Шквары, а также видоизмененными методами Коутса–Рэдферна и Бразейовски с сотр., с использованием метода наименьших квадратов для подгонки кривой. На первой стадии разложения преобладающими являются механизмы разложения A_2 и A_3, тогда как механизм F_1 лучше всего описывает дегидратацию структурной воды. Энергии активации, установленные для первой и второй стадий, равнялись, соответственно, 21 кдж · моль$^{-1}$ и 96 кдж · моль$^{-1}$.